

Elsevier required licence: © <2020>. This manuscript version is made available under the CC-BY-NC-ND 4.0 license <http://creativecommons.org/licenses/by-nc-nd/4.0/>
The definitive publisher version is available online at
[\[https://www.sciencedirect.com/science/article/pii/S004313542030511X?via%3Dihub\]](https://www.sciencedirect.com/science/article/pii/S004313542030511X?via%3Dihub)

19 **Abstract**

20 This study investigated the impacts of selective sole carbon source-induced micropollutants
21 (MPs) cometabolism of *Chlorella* sp. by: (i) extracellular polymeric substance (EPS),
22 superoxide dismutase and peroxidase enzyme production; (ii) MPs removal efficiency and
23 cometabolism rate; (iii) MPs' potential degradation products identification; and (iv)
24 degradation pathways and validation using the Eawag database to differentiate the
25 cometabolism of *Chlorella* sp. with other microbes. Adding the sole carbon sources in the
26 presence of MPs increased EPS and enzyme concentrations from 2 to 100-fold in comparison
27 with only sole carbon sources. This confirmed that MPs cometabolism had occurred. The
28 removal efficiencies of tetracycline, sulfamethoxazole, and bisphenol A ranged from 16-99%,
29 32-92%, and 58-99%, respectively. By increasing EPS and enzyme activity, the MPs
30 concentrations accumulated in microalgae cells also fell 400-fold. The cometabolism process
31 resulted in several degradation products of MPs. This study drew an insightful understanding
32 of cometabolism for MPs remediation in wastewater. Based on the results, proper carbon
33 sources for microalgae can be selected for practical applications to remediate MPs in
34 wastewater while simultaneously recovering biomass for several industries and gaining
35 revenue.

36 **Keywords:** cometabolism, micropollutant, microalgae, extracellular polymeric substance,
37 peroxidase

38

39 1. Introduction

40 Among thousands of micropollutants (MPs), tetracycline (TC), sulfamethoxazole (SMX), and
41 bisphenol A (BPA) are attracting many interests due to their widespread consumption. Up to
42 5500 tons of TC are consumed annually in the US and Europe (Ahsan et al., 2018). Notably,
43 50% of the used TC is released into the environment via human excretions; in the meantime,
44 TC appears in surface water in concentrations ranging from 0.11 to 4.2 µg/L (Ahsan et al.,
45 2018). The SMX of sulphonamide drug is used for bacterial disinfection and several medical
46 purposes. It especially targets the *Listeria monocytogenes* and *Escherichia coli*. However,
47 similar to TC, 10-50% of the consumed SMX is excreted via human waste into the
48 environment (Ahsan et al., 2018). Together with TC and SMX, BPA - a plasticizer chemical –
49 also receives much attention recently. BPA is utilized for epoxy resin, polycarbonate
50 polymers, and plastic fabrication. It resists biodegradation even though it only presents in
51 water at ppt level (Luo et al., 2014). Those toxic MPs need appropriate removal as current
52 wastewater treatment plants are ineffective in MPs removal (Luo et al., 2014). This waste
53 stream is a great risk to public health since it causes antibiotic-resistant genes in
54 microorganisms (Menz et al., 2019). Long term study has indicated those MPs also
55 accumulate in the food chain and drinking water, which threatens public health, especially
56 children (Wang et al., 2020).

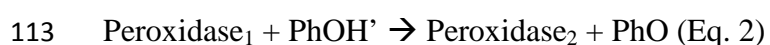
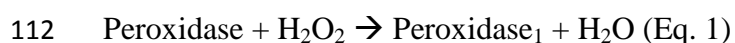
57 Despite chemical treatment proved to be useful for MPs removal, biological treatment is still
58 preferable because of its low-cost and biomass recovery. However, several MPs are poorly
59 biodegradable and toxic to the microbial consortium in wastewater treatment systems. In
60 practice, MPs exist at only small quantities in wastewater, they cannot participate in the
61 catabolic and anabolic processes of microbes. That is, bacteria are unable to consume those
62 compounds as sole carbon sources for building up cells. The received metabolic energy from
63 MPs is insignificant to microorganism. Thus, the sole and utilizable carbon substrates are

64 essential for the MPs biodegradation. Microorganism metabolizes the sole carbon sources
65 (e.g., carbonate, glucose, acetate) in wastewater and cometabolizes the MPs (Tran et al.,
66 2013). Cometabolism was initially proposed in the 1950s, which projected to the degradation
67 of chlorinated solvents and aromatic compounds. The cometabolism brings along potential
68 advantages. It triggers the conversion of persistent compounds to intermediates, which are
69 more biodegradable and readily participate in the metabolic pathways (Tran et al., 2013).
70 Therefore, cometabolism is a current approach to hazardous compounds removal.

71 Extracellular polymeric substances (EPS) and enzymes, which are excreted by
72 microorganisms, are the main catalysts of cometabolism. EPS adhere chemically and
73 physically onto several extracellular organic and inorganic substances thanks to their
74 functional groups (i.e., -COOH, -NH, -OH, -CO) (Xiao and Zheng, 2016). EPS can create a
75 hydrated biofilm which bind closely to the cells and function as an extracellular digestive
76 system. They facilitate the MPs cometabolism of various MPs forms such as dissolved,
77 colloidal, or solid ones. Protein and carbohydrate of EPS are charged and start accumulating
78 and cometabolizing MPs. EPS also serve as surfactant or emulsifier to condition the
79 bioavailability of MPs (Xiong et al., 2018). Previous studies have demonstrated that EPS and
80 enzymes of microorganism can remediate MPs and organic pollutants (Barajas-Rodriguez
81 and Freedman, 2018; Zhou et al., 2019). For example, the ammonia-oxidizing bacteria (e.g.,
82 *Nitrososphaera gargensis*, *Nitrosomomas nitrosa* Nm90, and *Nitrospira inopinata*) can
83 remediate seven sulphonamide compounds via particular enzymes. The typical enzymes are
84 ammonia monooxygenase, hydroxylamine dehydrogenase, and nitrite oxidoreductase (Zhou
85 et al., 2019). These enzymes degrade the sulphonamide compounds extensively, given that
86 none intermediates are detected. From those examples, it can be seen the cometabolism of
87 bacteria is understood increasingly recently. Nevertheless, little attention has been paid for
88 microalgae.

89 Microalgae have performed distinctively in terms of green technology. Unlike bacteria,
90 biomass of microalgae serves as feedstock for several industries such as fertilizer, stabilizing
91 substances (Nagarajan et al., 2020), supplementary drugs and bioenergy. Cultivating
92 microalgae in MPs-impacted wastewater can cut off extra costs of nutrient by reusing nutrient
93 in wastewater itself. It gains potential revenue. For instance, if microalgae biomass is
94 recovered from the wastewater treatment process, \$ 0.27 to \$ 1.80 per kg can be earned (Vo
95 Hoang Nhat et al., 2018). Biofuel production costs also diminish by \$0.55 to \$ 0.59 per liter
96 when using municipal wastewater to yield biomass of microalgae (Vo Hoang Nhat et al.,
97 2018). Thus, culturing microalgae in wastewater can remediate pollutants such as MPs and
98 also recover biomass for industries input. This concept provides both remediation and
99 economic benefits which could be referred as the “zero waste” one (Xiong et al., 2018). In
100 addition, microalgae can metabolize by both autotrophic and heterotrophic modes depending
101 on the available carbon sources in wastewater. This mechanism of microalgae metabolism
102 delivers substantial benefits compared to that of bacteria and fungi because microalgae are
103 more flexible and adapt well to the change of living conditions (Xiong et al., 2018). This is
104 the main momentum for studying MPs remediation by microalgae in wastewater.

105 Similar to bacteria, microalgae can secrete EPS and several types of hydrocarbon and protein.
106 *Chlorella* sp. is a common strain of microalgae that has been studied widely. It can excrete
107 several types of enzyme such as superoxide dismutase and peroxidase (Vo et al., 2020).
108 Those enzymes prime the cometabolism and degrade MPs. For example, peroxidase
109 participates in a cyclic reaction process of phenolic compound decontamination (Eq. 1-3),
110 which can catalyze the reaction of H₂O₂ and MPs to degradation products (Francoz et al.,
111 2015).



114 Peroxidase₂ + PhOH” → Peroxidase + PhO + H₂O (Eq. 3)

115 Our knowledge of cometabolism in microalgae towards MPs removal requires much more
116 attention. Several engineering aspects of cometabolism by microalgae also need to be
117 addressed (Xiao and Zheng, 2016). In general, cometabolism is influenced by a number of
118 factors (e.g., the solid retention time, originality of the MPs, microalgae strain, and nutrient
119 types) (Tran et al., 2013). Amongst them, the critical factor for cometabolism is the sole
120 carbon source type for microalgae growth. Several recent studies have indicated the influence
121 of some sole carbon sources on microalgae’s growth, including glucose, saccharose, acetate
122 and sodium bicarbonate (Moon et al., 2013; Tu et al., 2018; Vergnes et al., 2019; Wang et al.,
123 2016). For example, monosaccharides such as glucose and galactose at concentration of 1%
124 show a significant effect on *Chlorella pyrenoidosa* (Wang et al., 2016). They increase
125 carbohydrate levels in microalgae cells by 103.2–266.5% and 91.9–240.0%, respectively. On
126 the other hand, disaccharides and starch did not change the concentrations of lipid, protein
127 and carbohydrate in cells (Zhang et al., 2014). While the effect of carbon sources on the lipid,
128 protein and carbohydrate content is adequate, the mechanisms attributed to cometabolism and
129 MPs’ degradation products are still unknown. Previously, some studies investigated the
130 impact of different substrates on micropollutant cometabolism (Barajas-Rodriguez and
131 Freedman, 2018; Liang et al., 2011; Zhou et al., 2019). However, they are subjected to
132 aerobic and anaerobic bacteria, rather than microalgae. In practice, microalgae are applicable
133 for dealing with wastewater sources from slaughterhouses or pharmaceutical, beverage, and
134 textile industries (Bhattacharya et al., 2017; Cheng et al., 2019). Apart from sufficient
135 nitrogen and phosphorus, the sugar, alcoholic, acetate and other carbon sources in the
136 mentioned wastewater are essential nutrients for cultivating microalgae. The raising question
137 is how microalgae’s cometabolism respond to those carbon sources in terms of EPS excretion
138 and catalytic of relevant enzymes in extracellular and intracellular environments. Also, the

139 concern about MPs removal efficiency and MPs' degradation products also needs to be
140 elaborated.

141 To broaden scientific knowledge of cometabolism in microalgae, we investigated the effect of
142 different organic and inorganic carbon sources on the cometabolism of microalgae. The
143 evidence for MPs cometabolism was demonstrated by: (i) EPS and peroxidase enzyme
144 production, (ii) MPs removal efficiency and cometabolism rate; (iii) identifying the
145 degradation products of MPs, proposing degradation pathways; and (iv) validating findings
146 with the Eawag database to differentiate the cometabolism induced by *Chlorella* sp. and other
147 microbes. A comparison between Eawag's degradation pathways and our proposed pathways
148 proved the hypothesis that MPs' degradation products were formed differently based on the
149 microbes' strains. Overall, this study contributes towards the potential application for
150 industrial wastewater remediation by microalgae' cometabolism.

151 **2. Materials and methods**

152 2.1 Microalgae strain, artificial wastewater, and chemicals

153 The microalgae strain (*Chlorella* sp. CS-436) was supplied by the National Algae Supply
154 Service (Tasmania, Australia). The detail of microalgae cultivation was described in our
155 previous work (Vo et al., 2019b). Briefly, the microalgae stock was cultured in MLA media
156 (AusAqua, Australia), using constant temperature (20 ± 1 °C) and continuous illumination
157 intensity (4.35 ± 0.03 klux). The illumination intensity was recorded by a digital light meter,
158 model QM1584 (Digitech, Australia). The microalgae culture was subcultured by renewing
159 the medium every two weeks.

160 The experiment's artificial wastewater was prepared using different sole carbon sources:
161 methanol (CH_3OH), ethanol ($\text{C}_2\text{H}_5\text{OH}$), saccharose ($\text{C}_{12}\text{H}_{22}\text{O}_{11}$), glucose ($\text{C}_6\text{H}_{12}\text{O}_6$), sodium
162 acetate (CH_3COONa), glycine ($\text{C}_2\text{H}_5\text{NO}_2$), and sodium bicarbonate (NaHCO_3). They
163 included six organic and one inorganic carbon sources. Each carbon source was used

164 separately to create individual wastewater types. The trace vitamins (i.e., thiamine-HCl,
165 biotin, and B₁₂) were supplied by AusAqua Company (Australia) and dosed following the
166 supplier's instructions (1 mL vitamin for 1 m³ media). The used MPs included TC, SMX and
167 BPA and they were prepared in stocks of 1 g/L and diluted to the desired concentration. The
168 physico-chemical properties of those MPs are documented in Table S1. All the chemicals
169 were purchased from Merck (Australia) and of analytical grade quality.

170 2.2 Experimental designs

171 The photobioreactors used 1 L sealed glass bottles inoculated with 50 mg microalgae/L
172 concentration when the experiment started. The total used volume of each reactor was 900
173 mL to leave some space for the respiration of microalgae. The light intensity, temperature,
174 and vitamins were maintained at similar levels as what were applied during the culturing of
175 the stock. All the nutrient and MPs were added at day 0. Seven photobioreactors were added
176 with MLA media and each reactor possessed one sole carbon source as stated beforehand.
177 The initial concentration of total carbon (sole carbon source) in all reactors was 300 mg/L.
178 The control photobioreactor was also set up by adding MLA media and microalgae only (no
179 sole carbon source). The initial nitrogen (NaNO₃) and phosphorus (KH₂PO₄) in all reactors
180 were 30 mg/L and 5 mg/L, respectively. The control reactor was designed as a reference point
181 to evaluate the influence of sole carbon sources on the MPs' cometabolism. At the start, 20
182 µg/L each of BPA, SMX and TC were dosed in the eight photobioreactors. The experimental
183 period lasted 10 d in batch condition. The culturing solutions in photobioreactors were gently
184 stirred at 50 rpm to improve the exposure of microalgae, light, MPs and nutrients throughout
185 the whole experiment period.

186 2.3 Biomass yield, microalgae cells' morphology, elemental and total carbon analysis

187 The methods of biomass concentration, cell morphology, and elemental analysis were
188 described in the previous study (Vo et al., 2019b). To determine biomass yield, the optical

189 density (OD) of the sample at 680 nm was measured using a spectrophotometer (DR1900,
190 Hach) and converted to a biomass yield via Eq. 4. This wavelength was chosen since it was
191 the most sensitive to chlorophyll pigment of microalgae.

$$192 \quad y = 0.0021x + 0.0222 \quad (R^2 = 0.95) \quad (\text{Eq. 4})$$

193 Where, x: biomass concentration (mg/L), y: optical density

194 The cell morphology and elemental analysis of *Chlorella* sp. were conducted by Scanning
195 Electron Microscopy (SEM) and Energy Dispersive X-Ray Spectroscopy (EDS) (Zeiss Supra
196 55VP, Carl Zeiss AG), respectively. The sample was prepared following our previous works
197 (Vo et al., 2019b). The sample (10 mL) was filtered by a glass fiber filter paper GF/C
198 (Whatman, Australia), dried for 24 h at 105 °C in an oven and kept in a desiccator to maintain
199 vacuum conditions. Then it was coated using Au/Pd (10 nm thickness) with a Leica EM
200 ACE600 High Vacuum Sputter Coater. The coated sample was then imaged by SEM
201 operating at an accelerating voltage (10 kV), and multiple image magnifications were
202 produced for each sample (1000 to 5000x). The EDS characterized the C, N, and P
203 proportions in microalgae cells. The working distance of the electron beam was fixed at 10
204 mm. The I probe was adjusted accordingly to adjust the dead time from 3% to 10% to avoid
205 damage caused to the cell surface.

206 The total carbon concentration was analysed by Multi N/C 3100 (Analytikjena, Germany).

207 The sample was filtered by 1.2 µm Phenex-GF (Glass fiber) syringe filter, then diluted to fit
208 the threshold range of the equipment (100 mg/L).

209 2.5 Extracellular polymeric substances

210 The EPS extraction and analysis procedures were based on modifications of the methods used
211 by Deng et al. (2016) and Ni et al. (2009). A 30 mL sample was collected and centrifuged at
212 3000 rpm for 30 min then filtered through a 0.45 µm Phenex-NY (Nylon) syringe filter for
213 the soluble EPS. The remaining pellet was suspended in a phosphorus buffer solution to 30

214 mL and mixed with cation exchange resin (Dowex) for 2 h at 900 rpm. The bound EPS was
215 obtained by filtering the mixture through a 1.2 μm Phenex-GF (Glass fiber) syringe filter.
216 Each of the received soluble and bound EPS were analyzed for proteins and polysaccharides
217 concentrations using the Lowry method and Anthrone-sulphuric acid method, respectively.
218 The Lowry method was performed by the modified Lowry kit (Sigma, Australia).

219 2.6 Superoxide and peroxidase enzymes

220 The reactivity of superoxide dismutase (SOD) and peroxidase (POX) enzymes was analyzed
221 using SOD and POX assay kits (Sigma-Aldrich, Australia). Firstly, 20 mL sample was
222 collected and centrifuged at 4500 rpm for 15 min at 4 °C. The supernatant was used for the
223 enzymatic activity assay in the culturing environment. The pellet was washed three times and
224 filled up to 20 mL by Milli-Q water. The pellet sample was quickly frozen at -20 °C, thawed
225 at room temperature (37 °C), and then sonicated for 1 h following by centrifugation for 10
226 min at 4500 rpm. The supernatant was used for SOD and POX enzymatic activity in
227 microalgae cells. The SOD and POX analysis were conducted according to the manufacturer's
228 instructions. One SOD unit was defined as the amount of enzyme exhibited 50% dismutation
229 of the superoxide radical. The unit U/mL (nmol/min.mL) was used for SOD activity and the
230 unit nmol/h.mL was applied for POX activity.

231 2.8 MPs analysis

232 Microalgae were harvested by centrifugation at 4500 x g for 15 min. The supernatant was
233 used to determine the residual BPA, TC, and SMX in the medium. The cell pellets were
234 collected and gently washed three times using milli-Q water. The washing milli-Q portions
235 which contained MPs adsorbed to the surface of microalgae were collected (Ji et al., 2014). It
236 was mixed with the previous supernatant to identify the total MPs in the medium and
237 absorbed on the microalgae's surface. After washing, the pellet was collected and incubated
238 in 3 mL dichloromethane-methanol (1:2 v/v). The mixture was sonicated (350W, 50 Hz) for 1

239 h to assist cell lysis and centrifuged for 10 min at 4500 x g. The supernatant was used for
240 analyzing MPs in microalgae cells.

241 The samples were concentrated by solid phase extraction (SPE) using the Strata-X-C 33 µm,
242 Polymeric Strong Cation (Phenomenex, Australia). The analysis involved liquid
243 chromatography with mass spectrometry (LC MS 8060 Shimadzu), equipped with a Luna
244 Omega 3 µm Polar C18 column (Phenomenex, Australia). The MS was conducted with an
245 electrospray ionization (ESI) source (Thermo Fisher Scientific, USA). The ESI positive mode
246 was used for TC and SMX analysis while the ESI negative mode was applied for BPA. In
247 positive mode, the mobile A phase was Milli-Q water containing 0.1% formic acid and
248 mobile phase B was methanol. The gradient elution was performed at a constant flow rate
249 (0.4 mL/min) as follows: the mobile phase B was retained at 30% (0.01 to 0.29 min),
250 increased to 95% (0.29 to 7 min), and then decreased to 30% (7 to 7.5 min). The multiple
251 reaction modes (MRMs) of SMX (254.1>156, 254.1>92) and TC (445.25>410, 445.25>428)
252 were selected. In negative mode, the mobile phase A was Milli-Q water while the mobile
253 phase B and flow rate were the same as in positive mode. The gradient elution was: the
254 mobile phase B rose from 25% to 95% (0.01 to 2 min), held at 95% (2 to 6.5 min), and then
255 declined to 25% (6.5 to 7 min). The MRM modes of BPA were 227.1>133 and 227.1>212.
256 The internal standards of the negative mode (diclofenac) and positive mode (sulfadiazine)
257 were spiked at a concentration of 2 µg/L to guarantee the analytical quality.

258 2.9 Degradation products analysis

259 Samples for degradation products screening were prepared in the same way described in
260 section 2.8. The potential degradation products of the contaminants were investigated using
261 LC-HRMS system consisted of an Agilent 1290 Infinity LC coupled with an Agilent 6550
262 iFunnel QTOF equipped with a Dual Spray ESI source. Chromatographic separation was
263 obtained by an Accquity UPLC BEH column (2.1 x 100mm, 1.7µm, Waters, U.S.A) with

264 water as mobile phase A and methanol as mobile phase B. The eluting gradient was according
265 to Table S2. Each sample was analyzed twice, once in negative and once in positive ESI
266 mode. The obtained data were screened against a local library consisted of potential
267 degradation products reported previously in the literature using Mass Hunter software
268 (Agilent, U.S.A). The mass accuracy was set to 5 ppm and isotope pattern scoring was
269 applied. Instrumental blanks (pure methanol) were analyzed between every 5 samples.

270 The degradation products and degradation pathways were also proposed using the Eawag-
271 Biocatalyst/Biodegradation Database Pathway Prediction System (Eawag-BBD) (Eawag,
272 2019). This platform predicted the biotransformation of MPs based on published literature. In
273 this study, we enabled the MPs degradation pathways of Eawag-BBD by focusing on the
274 aerobic conditions, which were closely linked to the microalgae. The degradation pathways
275 hierarchy and degradation products at each level were established at 3 and 5, respectively.

276 2.10 Cometabolism rate ($K_{\text{cometabolism}}$) estimation

277 During the MPs' cometabolism, other mechanisms occurred and typically these were
278 volatilization and adsorption. However, both volatilization and adsorption played a minor role
279 overall. The three MPs had low partitioning coefficients (below 500 L/kg) and octanol-
280 water coefficients (less than 1) which made them hydrophilic and resistant to the adsorption
281 process. The volatilization of MPs was calculated via Henry's constant. A value that was
282 higher than 10^{-3} meant the compound was considered volatile. The Henry's constant of the
283 MPs was less than 10^{-5} and this indicated they were highly retained in water. Thus, the
284 adsorption and volatilization were minor issues in this study, while cometabolism contributed
285 significantly. The cometabolism rate of selected MPs could be described via the pseudo first-
286 order kinetics as previously in another study (Park et al., 2017)

$$287 \frac{dC}{dt} = -k \times C \Leftrightarrow C_t = C_0 \times e^{-kt} \text{ (Eq. 5)}$$

288 Where k was the first-order rate constant (1/h), C_t was the MPs concentration ($\mu\text{g/L}$) at time t
289 (h), and C_0 was the initial MPs concentration ($\mu\text{g/L}$).

290 2.11 Statistic analysis

291 The analyses of variance (ANOVA) were used for statistical investigation. The repeated
292 ANOVA measures were applied to examine the significant difference in biomass yield
293 according to different carbon sources. Concentrations of EPS, enzymes, and MPs in aqueous
294 phase and cells were presented as mean (standard deviation). All the statistical analyses were
295 processed using Origin 2017 (Origin Lab, USA) software at 95% confidence level.

296 3. Results and discussion

297 3.1. Variation of biomass culturing by different sole carbon sources and micropollutants

298 Types of carbon sources and MPs impacted differently on the growth of *Chlorella* sp. Based
299 on the received biomass yield, we classified the influence of carbon sources into three groups:
300 high, moderate, and low-yield one (Fig. 1a). The high-yield group included glucose and
301 saccharose. This group achieved biomass higher than 700 mg/L after 10 d. The moderate-
302 yield group possessed glycine, sodium acetate and sodium bicarbonate. For this group, the
303 biomass varied from 300 to 700 mg/L. The biomass concentration of bicarbonate and glycine
304 samples was higher than that of the acetate one 100 mg/L. The low-yield group consisted of
305 methanol and ethanol with biomass concentration under 300 mg/L. This value was less than
306 the one of the high-yield group from 4 to 7 times.

307 The advanced techniques (i.e., SEM and EDS) were also used to investigate the influence of
308 the sole carbon sources and MPs on biomass (Fig. 1b, c, d, e, and Table 1). By culturing
309 microalgae with methanol, the shape of microalgae cells became a “flattened balloon”. This
310 happened similarly to the control sample. For ethanol, although cells density was low, they
311 looked stronger than the one cultured by methanol and the control sample. In turn, the cells
312 cultured by carbon sources in the moderate and high-yield groups differed from the low-yield

313 group. Those cells' shape remained dense and full which could be observed clearly. The SEM
314 images agreed with the data of microalgae biomass because more cells were found in the
315 high-yield group and vice versa.

316 [Insert Fig. 1]

317 Through the EDS technique, we demonstrated the C, N and P percentages in microalgae cells
318 which impacted by different carbon sources and MPs (Table 1). We analysed the C:N:P ratios
319 and the results performed consistently with the data of biomass concentrations and addressed
320 the discrepancies in C percentages. Compared with the optimal C:N:P ratio, so-called
321 Redfield ratio, we discovered that the ratios of glucose and saccharose-feeding samples were
322 close to the Redfield ratio. They differed by only 5-10% which was acceptable. The low-yield
323 group was 50% less than the Redfield ratio. Also, the C:N:P ratios for the moderate group
324 varied from 20% to 40% compared to the Redfield ratio. Accordingly, the data of EDS re-
325 confirmed the consistent effect of carbon sources and MPs on the growth of *Chlorella* sp.

326 [Insert Table 1]

327 3.2. Sole carbon sources consumption, extracellular polymeric substances and enzymes
328 production for cometabolism

329 Microalgae can accumulate C for building up cells which is critical to produce biomass, EPS,
330 and enzymes. By using 300 mg carbon/L, we studied the sole C assimilation of *Chlorella* sp.
331 over 10 d (Fig. 2a). Consequently, the low-yield group removed the sole C insufficiently at
332 less than 30%. On the contrary, the moderate and high-yield groups can accumulate more
333 than 70% to 90% of the sole C. This indicated that microalgae consumed those sole carbon
334 sources for the purposes of metabolism; then it started producing EPS and enzymes for the
335 cometabolism of MPs (see sections 3.5 - 3.6). The outcome of C assimilation also suggested
336 applicability for industrial wastewater remediation (discuss in section 4).

337 Generally, the EPS concentration ranged from 10 to 30 mg/L (Fig. 2b). Most of the carbon
338 sources impacted positively on microalgae by excreting more EPS. Glucose, saccharose, and
339 glycine induced microalgae producing the highest amount of EPS, up to 30 mg/L. These EPS
340 levels surpassed the ones of alcohol-culturing microalgae by 2- to 3-fold. In details of the
341 EPS composition, the amount of carbohydrate was 3 - 98 times less than protein. For protein
342 produced by methanol, ethanol, glycine and bicarbonate carbon sources, the concentration of
343 the bound form was equal to the soluble one. The bound protein which subjected to glucose
344 and saccharose carbon source exceeded the soluble protein by 2 to 3 times. It can be seen that
345 bound protein is the major compound of EPS excreted by microalgae.

346 The SOD and POX enzymes were produced both in the culturing liquid and microalgae cells
347 (Fig. 2c, d). SOD and POX were the key enzymes for EPS regulation of stress alleviation and
348 they reflected the MPs' cometabolism. The SOD concentration in microalgae cells, when
349 cultured by sodium acetate and glycine, ranged from 30 to 40 U/mL. Other carbon sources
350 demonstrated similar SOD levels in the cells compared to the medium. However, the
351 concentrations of SOD in both environments were still 2 to 6 times higher than the control
352 samples. For POX, it was produced less 6 nmol/h.mL which was lower than that of SOD.
353 These concentrations tripled the amounts presented in the microalgae cells.

354 To sum up, in this section we found that microalgae consumed carbon sources and excreted
355 EPS in the culturing environment. In addition, SOD and POX enzymes were also detected in
356 both the culturing environment and cells. Microalgae which cultured in glucose and
357 saccharose possessed the highest EPS and enzyme concentrations.

358 [Insert Fig. 2]

359

360 3.3 How carbon sources impact on microalgae?

361 From sections 3.1 and 3.2, it can be seen that biomass concentration, cell morphology, EPS,
362 and enzyme productivities of microalgae were influenced by carbon sources and MPs. In this
363 section, we discussed the impact of carbon sources on microalgae and cometabolism
364 processes insightfully, using scientific evidences of biochemistry studies. In brief, there were
365 two plausible reasons: energy content of carbon sources and metabolic pathways of
366 microalgae (Vo et al., 2020).

367 The studied carbon sources possessed energy content at various degrees. For example,
368 saccharose, glucose, and acetate had energy contents at 4.2, 2.8 and 0.8 kJ energy/mol,
369 respectively (Perez-Garcia et al., 2011). This explained why saccharose and glucose yielded
370 the highest biomass concentrations, EPS and enzymes compared to acetate. In turn, the
371 alcoholic carbon sources (e.g., methanol and ethanol) wielded lower energy pools of 0.1
372 kJ/mol and 0.5 kJ/mol, respectively (Cardol et al., 2011). This confirmed the low level of
373 biomass and related products of microalgae culturing by alcoholic carbon sources (Fig. 1).

374 Consuming carbon sources by various metabolic pathways is another explanation for the
375 discrepancy of biomass yield, cell morphology and related products. The involved metabolic
376 pathways for those carbon sources include Embden–Meyerhof Pathway (EMP), tricarboxylic
377 acid (TCA), Glyoxylate Cycle and Calvin Cycle.

378 The EMP and TCA cycles involved in the metabolism of sugar-based carbon sources. In
379 detail, microalgae metabolized glucose by the EMP and the TCA cycles to produce ATP.
380 Likewise, microalgae consumed saccharose by catalytic enzymes that degraded saccharose to
381 monomers (i.e., glucose and fructose) (Wang et al., 2016). The monosaccharides were then
382 uptaken and transported by the EMP and the TCA cycles. Via the EMP and TCA cycles, cells
383 only used one ATP to transport one sugar molecule (Perez-Garcia et al., 2011). Those cycles
384 could also convert sugar molecules into phosphoanhydride bonds of ATP for storing energy

385 pool. The conversion efficiency reached up to 12%. Thus, by consuming fewer ATP pools
386 and storing energy effectively, cells could generate more biomass, EPS and enzyme for co-
387 metabolism. The cell morphology was also full-filling for the same reason.

388 Unlike the sugar carbon sources, acetate involved in the Glyoxylate Cycle for lipid
389 production prior to being metabolized in the TCA cycle. This diminished acetate stock
390 available for biomass, EPS, and enzyme production. Bouarab et al. (2004) stated that glucose
391 contributed 38 moles of ATP whereas acetate gave 12 moles for microalgae growth. This
392 clarified the productivities of microalgae culturing in acetate were less than glucose and
393 saccharose. Similarly, glycine contained an amino group (-NH₂), which particularly served
394 for chlorophyll and carotene production (Cecchin et al., 2018). This process also reduced
395 glycine stock for biomass, EPS and enzymes production. Likewise, inorganic carbon source
396 produced less biomass, EPS and enzymes because photoautotrophic performed less effective
397 than the heterotrophic and mixotrophic modes (Yeh and Chang, 2012). The reason attributed
398 to the Calvin cycle. In the autotrophic mode, it used 70% ATP stock and produced 3.11 g
399 biomass/mmol ATP. In turn, it yielded 19.3 g biomass/mmol ATP in the heterotrophic and
400 mixotrophic modes (Yang et al., 2000). For the alcohol carbon sources, microalgae lost ATP
401 substantially because they used ATP to repair the damage caused by those carbon sources.
402 The lost amount reached up to 45 – 82% of the total ATP pool (Yang et al., 2000). This also
403 explained why the morphology of cells was flat in alcoholic carbon sources.

404 3.4 Proof of micropollutants' cometabolic degradation

405 As the TC, SMX, and BPA (20 µg/L each) were dosed together with different carbon sources,
406 the microalgae cometabolized those MPs in different ways. The efficiencies in removing TC,
407 SMX and BPA ranged from 16-99%, 32-92% and 58-99%, respectively (Fig. 3a, b). Without
408 adding carbon sources, the removal efficiencies of the control samples were 27-41%, which
409 was half that of adding carbon sources. This evidence, together with the increase of EPS and

410 enzyme level after adding carbon sources, confirmed that the MPs' removal was due to
411 cometabolic transformation. It is because the additional carbon sources could participate in
412 the cometabolism of MPs as electron donors. They also conditioned the increasing release of
413 catabolic enzymes for degrading MPs, such as EPS, SOD and POX of this study (Xiong et al.,
414 2018). By the stress of both carbon sources and MPs to the reactive oxygen species system,
415 microalgae excreted EPS and several enzymes as self-defensive react.

416 In the culturing liquid, the glucose-cultivating microalgae achieved the highest MPs removal
417 efficiency, which was above 80% for all MPs. The saccharose and glycine-culturing
418 microalgae also removed large amounts of MPs, greater than 90% for at least two MP types.
419 Other carbon sources, namely methanol, ethanol, acetate, and bicarbonate removed more than
420 90% of only one MP. Specifically, the acetate-cultivating microalgae only cometabolized
421 16% of TC. Overall, TC and BPA were degraded efficiently in all bioreactors at $91 \pm 15\%$
422 ($n=6$) and $81 \pm 17\%$ ($n=7$), respectively. The removal efficiency of SMX was somewhat less
423 efficient at $66 \pm 25\%$ ($n=7$).

424 For MPs that had accumulated in microalgae, adding carbon sources reduced their
425 intracellular concentrations compared to those without a carbon source. Without adding a
426 carbon source, the concentrations of TC, SMX, and BPA in microalgae cells were 425.8,
427 480.8 and 88.3 ng/mg, respectively (Fig. 3c). By adding the carbon sources, the accumulated
428 MPs' concentration diminished 400-fold, and an insightful discussion on this decrease was
429 documented in section 3.6. Of the three MPs related the sole carbon sources, microalgae
430 accumulated TC the most (23.2 ± 32.0 ng/mg). It was 10 to 20 times higher than the
431 accumulated concentrations of SMX and BPA, these being 1.12 ± 1.87 and 2.69 ± 2.89
432 ng/mg, respectively (Fig. 3d).

433 [Insert Fig. 3]

434 The cometabolism rate of MPs ($K_{\text{cometabolism}}$) was estimated in Table 2. According to Joss et
435 al. (2006), $K_{\text{cometabolism}}$ less than 0.1/d implicates minimal removal of MPs, in fact less than
436 20%. In turn, the $K_{\text{cometabolism}}$ exceeded 0.1/d suggested that the cometabolism degradation
437 was significant. The $K_{\text{cometabolism}}$ values and MPs' removal efficiencies of this study agreed
438 with other analyses (Joss et al., 2006; Park et al., 2017). Most of the $K_{\text{cometabolism}}$ of SMX was
439 less than 0.1/d which persisted throughout the low SMX removal efficiencies. Only the
440 $K_{\text{cometabolism}}$ of glucose- and saccharose-culturing microalgae varied from 0.1 to 0.4/d and this
441 range indicated a significant amount of MPs being removed. This showed glucose and
442 saccharose cometabolized MPs the most efficiently.

443 [Insert Table 2]

444 3.5 How micropollutants influence on microalgae?

445 In this section, we explained in detail the impact of MPs on the EPS and enzymes production
446 of microalgae, which play a key role in MPs' cometabolism. By comparing the results of
447 using non-MPs carbon sources to culture microalgae, we found that the impact of MPs on
448 EPS and enzyme generation was significant (Vo et al., 2020). The EPS concentration
449 increased 2 to 4-fold for most carbon sources after adding MPs (Table S3). The concentration
450 of POX also rose by 20 to 100 times while using MPs rather than non-MPs environments. In
451 contrast, the concentration of SOD in both liquid and cells of MPs-cultured microalgae
452 declined 2 to 20 times. Microalgae excreted EPS, which contained various types of enzymes,
453 not restricted only to SOD and POX. It might include catalase, malondialdehyde, glutathione
454 S-transferase (GST), and Cyt P450 (Wang et al., 2018; Xiong et al., 2017). The detection of
455 all enzymes in EPS was technically difficult but this suggested that many more unknown
456 enzymes might participate in the MPs' degradation. For instance, GST could catalyze the
457 conjugation of reduced glutathione to various substrates, encompassing MPs (Tang et al.,
458 1998).

459 The SOD enzyme constructed the first line of defense against reactive oxygen species. It
460 catalyzed O_2^- to H_2O_2 and reduced toxicity to cells. Technically, under pressure from the
461 MPs, microalgae increasingly excreted SOD to alleviate the stress. However, in this case, the
462 spiked MPs concentration exceeded the tolerable threshold of microalgae and it led to a
463 decrease of SOD concentration. This outcome agreed with findings from previous studies
464 (Sun et al., 2018; Xiong et al., 2019). For instance, one agricultural crop could not produce
465 SOD when the MPs' concentration was higher than 5 $\mu\text{g/L}$ (Sun et al., 2018). Some MPs (i.e.,
466 triclosan and galaxolide) possessed high toxicity that interfered with the SOD's functioning.
467 In this study, we used TC, SMX and BPA which also possessed high toxicity (Xiong et al.,
468 2019). The EC_{50} value of SMX and triclosan were 0.12 mg/L and 0.39 mg/L, respectively
469 (Orvos et al., 2002). However, microalgae can tolerate high-dose of some chemicals i.e.,
470 ciprofloxacin, in fact up to 100 mg/L (Xiong et al., 2016). In this case, microalgae consumed
471 the MPs as the sole carbon source; however, the generated SOD did not exceed 2 U/g. This
472 meant that the SOD system of microalgae suffered differently according to the types of MP.
473 By increasing the amount of MPs, H_2O_2 was accumulated substantially and exceeded the
474 detoxification level of the SOD system, which explained the SOD inhibition.

475 Unlike the SOD system, microalgae excreted more POX when exposed to MPs, thus
476 indicating the adaptation and resistance of the POX system to MPs. This POX enzyme
477 catalysed the reaction using H_2O_2 for the degradation of MPs (Eq.1 - 3). For instance, it could
478 oxidize xenobiotics such as diclofenac and estradiol (Huber et al., 2016; Li et al., 2017).
479 Generation of POX was studied in plants and bacteria but very limited in microalgae.
480 Compared to plants and bacteria, the POX concentration of microalgae was relatively smaller.
481 For example, *Scirpus validus* could produce 0.5 U/g while exposed to hospital wastewater
482 containing 10 mg acetaminophen/L (Vo et al., 2019a). *Pseudomonas* spp. and *Bacillus* spp.
483 also produced 1.4 U/mL while being subjected to 100 mg BPA/L (Moussavi and Abbaszadeh

484 Haddad, 2019). Thus, we hypothesized POX contributed to the MPs' cometabolism as shown
485 in Fig. 4.

486 3.6 Degradation products of MPs induced by cometabolism

487 Although MPs were cometabolized efficiently, their fate and transformation need to be
488 explored in more detail. To identify the degradation products of MPs, the suspected screening
489 was conducted in both the culturing liquid and microalgae cells. We focused on the
490 degradation products of cometabolism culturing in saccharose since the EPS and enzymes of
491 this carbon source received the highest level. Based on the established criteria (section 2.9),
492 we only detected the degradation products of BPA as illustrated in Table 3. A possible reason
493 was that both TC and SMX were degraded to the degradation products, which were not in the
494 suspected list. Or else, the degradation products presented at concentrations below the
495 detection limit and did not satisfy the screening criteria.

496 SMX and TC were antibacterial agents and could be degraded by some possible enzymes. For
497 instance, the cytochrome c and membrane-bound hydrogenases are known to be involved in
498 SMX degradation (Gonzalez-Gil et al., 2019). They catalyzed feroxidase, an iron-sulphur
499 protein, reducing N-O bond of isoxazole ring in SMX. In addition, SMX can react with aryl-
500 acylamidases (EC 3.5.1.13) due to the strong reactivity of mono- or unsubstituted anilide
501 substructures. In one recent report, the cometabolic degradation of SMX was subjected to
502 three degradation products consisting of masses of 237, 239, and 300 (Zhou et al., 2019).
503 They underwent deamination, hydroxylation and nitration mechanisms and produced nitro
504 and hydroxyl groups. In those studies, the degradation products of SMX were not detected in
505 the intracellular environment and Zhou et al. (2019) indicated that no active uptake of SMX
506 happened. However, we detected SMX in microalgae cells.

507 In both positive and negative modes of LC-HRMS, the detected degradation products were
508 mostly from BPA which possessed masses of 163.07, 261.11, 153.09, 133.06 and 253.21

509 (denoted as “P163”, “P261”, “P153”, “P133” and “P253”), respectively (Fig. S1 – S5). Based
510 on accurate masses of the degradation products, we proposed the structure of degradation
511 products accordingly. It can be seen that four of them were scavenged by the oxidation
512 process. Three degradation products consisted of one benzene ring, while the other benzene
513 ring derived from BPA molecules was totally scavenged. The substance methyl cinnamate
514 was probably a product of peroxidase enzyme oxidation. Previously, it was detected after
515 laccase oxidation in a fungal reactor (Daâssi et al., 2016). The peroxidase and laccase were
516 the enzymes of a similar oxidoreductase class. The degradation of BPA did not occur
517 completely since some degradation products had larger masses compared to the parents, such
518 as P261 and P253. For the P261, perhaps after the benzene ring was broken, the hydroxyl
519 radical group continually encountered the opened C chain and bound the O atom to the chain.
520 Also, the straight C chain of the P253 resulted from the opening of two benzene rings. Those
521 proposed structures needed confirmation by using reference standards. However, such
522 standards were not commercially available so the given structures remain hypothetical (Yu et
523 al., 2018).

524 Based on the detected peak areas, the P133 and P253 were likely the dominant degradation
525 products out of five. P133 was the main degradation product in the culturing liquid, whereas
526 P253 governed the intracellular one. Their peak intensities surpassed the ones of P163, P261,
527 and P153 by 10 to 80-fold. In the intracellular of microalgae cells, both the benzene rings of
528 BPA molecules were cleaved to straight chain degradation products of P253. The high-
529 intensity straight chain product indicated an on-going detoxification process undertaken by
530 cometabolism. We did not detect any straight-chain degradation products in the culturing
531 liquid.

532

[Insert Table 3]

533 Based on the hypothetical structure of BPA degradation products, we proposed the
534 cometabolic degradation pathway as shown below (Fig. 4). At first, the hydroxyl radical
535 group ($\bullet\text{OH}$) of enzymes encountered various positions in the BPA molecules. The P261 was
536 formed while the $\bullet\text{OH}$ scavenged the C6 and C6' of the two aromatic rings. The C6 and C6'
537 were likely the weakest positions in BPA molecules since the values of the "highest occupied
538 molecular orbital" were the highest (Zhao et al., 2018). It meant they were the most active
539 ones for the $\bullet\text{OH}$ scavenger. In the meantime, the transient radical ($^*\text{C}(\text{CH}_3)_2\text{C}_6\text{H}_4\text{OH}$, C) was
540 created and rapidly turned into P133. In the next step, the P261 was divided into aromatic
541 ring degradation products, including P153, while the connecting C of the two rings was
542 cleaved. This degradation pathway agreed with Zhao et al. (2018) who studied BPA
543 degradation by the $\bullet\text{OH}$ scavenger. The contribution of the $\bullet\text{OH}$ group to the cometabolic
544 enzyme in this study was thus confirmed. For the P163 and P253, the degradation pathway
545 was complicated. Although these degradation products have been investigated (Sarma et al.,
546 2019), their degradation pathways remained unclear. Unlike the P253, the P163 was not
547 considered to be the final product since the ester group could be displaced from the ring and
548 oxidized into more simple products. This explained why the peak area of the P163 was lower
549 than that of the P253.

550 [Insert Fig. 4]

551 To validate the proposed degradation pathway, we used the Eawag-
552 Biocatalyst/Biodegradation Database Pathway Prediction System (Eawag-BBD) and obtained
553 another degradation pathway as depicted in Fig. 5. This degradation pathway included typical
554 enzymes such as phenol 2-monooxygenase (denoted bt0014), bisphenol A-hydrolase (denoted
555 bt0225), and bisphenol A-1-monooxygenase (denoted bt0436) for breaking the bonds of the
556 two aromatic rings. For example, the bisphenol A-hydrolase catalyse bisphenol A compound
557 transformed into 1,2-bis(4-Hydroxyphenyl)-2-propanol (product 2 in Fig. 6) when it received

558 H^+ from NADH. Later on, the extradiol or an extradiol-type enzyme (denoted bt0357) opened
559 the ring and formed maleylacetate (product 6 in Fig. 5), succinate (product 10 in Fig. 5) and
560 other derivatives (products 11, 12 in Fig. 5). Technically, our degradation pathway and the
561 one in the Eawag-BBD agreed on the gradual breakdown of BPA compound into simpler
562 products. Some of the degradation products were apparently similar. For example, our P163
563 and product 7 of Eawag-BBD only differed in terms of one OH group at the side chain of the
564 aromatic ring. This was because the $\bullet OH$ group continually struck the side chain.
565 Nonetheless, the P133 in this study and product 9 of Eawag-BBD only differed in the $=CH_2$
566 and $=O$ functional groups being at the side chain. The Eawag-BBD database was constructed
567 from a huge set of aerobic microbes, whereas our degradation products were derived from
568 microalgae cometabolism. This resulted in only a slight variation in the degradation products'
569 structures.

570 [Insert Fig. 5]

571 **4. Implications for wastewater remediation**

572 This study highlighted the potential for industrial wastewater remediation. For instance, the
573 chemical, pharmaceutical, aquaculture, and cattle industries discharge millions of cubic
574 meters of wastewater every year (Bhattacharya et al., 2017; Cheng et al., 2019). Those waste
575 streams brought with them various carbon sources, for example, sugar, acetate, and alcohol-
576 based which were beneficial for microalgae cultivation. Glycine and acetate were also part of
577 the amine-rich wastewater, released from the degradation of amine-based adsorbent (Dong et
578 al., 2019). In addition, those streams also contained MPs such as antibiotics, hormones and
579 sulphonamide, which infiltrated the chemical production process, food fed to cattle and
580 aquatic animals. By culturing microalgae in those wastewater sources, nutrients and valuable
581 pigment such as chlorophyll and carotene could be recovered. Simultaneously, MPs were able
582 to be partially removed via cometabolism.

583 Despite the fact that microalgae could efficiently degrade some investigated MPs in this
584 study, the metabolism pathways were still not fully discovered and understood. It was
585 important to further explore the transformation pathways of MPs in the cometabolism
586 process. As well, the related enzymes also required an in-depth investigation. In practice, the
587 wastewater matrix was complex because it contained many inhibitors. The degradation
588 products' transformation might occur in unpredictable ways and enzyme activity could be
589 diminished.

590 Based on the above results, recalcitrant compounds like SMX were not removed efficiently.
591 Thus, several alternatives could be considered to handle the issue: (i) using external enzyme
592 sources, (ii) adding cofactors to increase enzyme activity, and (iii) using metabolic
593 engineering. The external peroxidase sources could improve enzyme activity and accelerate
594 the MPs' degradation rate. External peroxidase could be obtained from various sources, such
595 as soybean and horseradish (Duarte Baumer et al., 2018; Moussavi and Abbaszadeh Haddad,
596 2019; Tavares et al., 2018). The enzyme could be doped on materials (i.e., activated carbon,
597 ferroxite nanoparticles) or presented in the free-enzyme form. Alternatively, cofactors
598 helped to enhance cometabolic efficiency. The natural mediators included syringaldehyde,
599 acetosyringone, and vanillin. For instance, MPs' degradation increased by 60 - 95% while
600 using the cofactors (Nguyen et al., 2014).

601 **5. Conclusion**

602 The understanding of cometabolism in microalgae is still limited. This study documents proof
603 that MPs can be cometabolized by microalgae fed by different sole carbon sources. We have
604 demonstrated the evidence for the following: (i) sole carbon sources' consumption and their
605 effects on biomass; (ii) EPS and enzyme generation; (iii) MPs' cometabolism; and (iv) MPs'
606 degradation products and proposed certain degradation pathways. This offers very useful and
607 practical insights into MPs' cometabolism by microalgae. The experimental data also

608 suggested that various enzyme types are involved in the MPs' cometabolism process, but not
609 only SOD and POX, which need further detailed investigation. Finally, the degradation
610 products of microalgae's cometabolism included the straight-chain version, which differed
611 from other microbes in the Eawag database.

612

613 **Acknowledgement**

614 This research was supported by the Centre for Technology in Water and Wastewater,
615 University of Technology, Sydney, Australia (UTS, RIA NGO) and the Korea Institute of
616 Energy Technology Evaluation and Planning (KETEP) and the Ministry of Trade, Industry &
617 Energy (MOTIE) of the Republic of Korea (Grant No. 20173010092470).

618

619 **References**

- 620 1. Ahsan, M.A., Islam, M.T., Hernandez, C., Castro, E., Katla, S.K., Kim, H., Lin, Y.,
621 Curry, M.L., Gardea-Torresdey, J., Noveron, J.C., 2018. Biomass conversion of saw dust
622 to a functionalized carbonaceous materials for the removal of Tetracycline,
623 Sulfamethoxazole and Bisphenol A from water. *J. Environ. Chem. Eng.*, 6 (4), 4329-
624 4338.
- 625 2. Barajas-Rodriguez, F.J., Freedman, D.L., 2018. Aerobic biodegradation kinetics for 1,4-
626 dioxane under metabolic and cometabolic conditions. *J. Hazard. Mater.*, 350, 180-188.
- 627 3. Bhattacharya, S., Pramanik, S.K., Gehlot, P.S., Patel, H., Gajaria, T., Mishra, S., Kumar,
628 A., 2017. Process for Preparing Value-Added Products from Microalgae Using Textile
629 Effluent through a Biorefinery Approach. *ACS Sustain. Chem. Eng.* 5(11), 10019-10028.
- 630 4. Bouarab, L., Dauta, A., Loudiki, M., 2004. Heterotrophic and mixotrophic growth of
631 *Micractinium pusillum* Fresenius in the presence of acetate and glucose:effect of light
632 and acetate gradient concentration. *Water Res.*, 38 (11), 2706-2712.

- 633 5. Cardol, P., Forti, G., Finazzi, G., 2011. Regulation of electron transport in microalgae.
634 *Biochimica et Biophysica Acta (BBA) - Bioenergetics* 1807 (8), 912-918.
- 635 6. Cecchin, M., Benfatto, S., Griggio, F., Mori, A., Cazzaniga, S., Vitulo, N., Delledonne,
636 M., Ballottari, M., 2018. Molecular basis of autotrophic vs mixotrophic growth in
637 *Chlorella sorokiniana*. *Sci. Rep.*, 8 (1), 6465.
- 638 7. Chen, B., Li, F., Liu, N., Ge, F., Xiao, H., Yang, Y., 2015. Role of extracellular
639 polymeric substances from *Chlorella vulgaris* in the removal of ammonium and
640 orthophosphate under the stress of cadmium. *Bioresour. Technol.*, 190, 299-306.
- 641 8. Cheng, D.L., Ngo, H.H., Guo, W.S., Chang, S.W., Nguyen, D.D., Kumar, S.M., 2019.
642 Microalgae biomass from swine wastewater and its conversion to bioenergy. *Bioresour.*
643 *Technol.*, 275, 109-122.
- 644 9. Daâssi, D., Prieto, A., Zouari-Mechichi, H., Martínez, M.J., Nasri, M., Mechichi, T.,
645 2016. Degradation of bisphenol A by different fungal laccases and identification of its
646 degradation products. *Int. Biodeterior. Biodegrad.*, 110, 181-188.
- 647 10. Deng, L., Guo, W., Ngo, H.H., Du, B., Wei, Q., Tran, N.H., Nguyen, N.C., Chen, S.-S.,
648 Li, J., 2016. Effects of hydraulic retention time and biofloculant addition on membrane
649 fouling in a sponge-submerged membrane bioreactor. *Bioresour. Technol.*, 210, 11-17.
- 650 11. Dong, C., Huang, G., Cheng, G., An, C., Yao, Y., Chen, X., Chen, J., 2019. Wastewater
651 treatment in amine-based carbon capture. *Chemosphere*, 222, 742-756.
- 652 12. Duarte Baumer, J., Valério, A., de Souza, S.M.A.G.U., Erzinger, G.S., Furigo, A., de
653 Souza, A.A.U., 2018. Toxicity of enzymatically decolored textile dyes solution by
654 horseradish peroxidase. *J. Hazard. Mater.*, 360, 82-88.
- 655 13. Eawag, Biocatalyst/Biodegradation Database Pathway Prediction System, URL:
656 <http://eawag-bbd.ethz.ch/acknowledge.html>. Access: 11 November 2019.

- 657 14. Francoz, E., Ranocha, P., Nguyen-Kim, H., Jamet, E., Burlat, V., Dunand, C., 2015.
658 Roles of cell wall peroxidases in plant development. *Phytochemistry*, 112, 15-21.
- 659 15. Gonzalez-Gil, L., Krah, D., Ghattas, A.-K., Carballa, M., Wick, A., Helmholz, L., Lema,
660 J.M., Ternes, T.A., 2019. Biotransformation of organic micropollutants by anaerobic
661 sludge enzymes. *Water Res.*, 152, 202-214.
- 662 16. Huber, C., Preis, M., Harvey, P.J., Grosse, S., Letzel, T., Schröder, P., 2016. Emerging
663 pollutants and plants – Metabolic activation of diclofenac by peroxidases. *Chemosphere*,
664 146, 435-441.
- 665 17. Ji, M.-K., Kabra, A.N., Choi, J., Hwang, J.-H., Kim, J.R., Abou-Shanab, R.A.I., Oh, Y.-
666 K., Jeon, B.-H., 2014. Biodegradation of bisphenol A by the freshwater microalgae
667 *Chlamydomonas mexicana* and *Chlorella vulgaris*. *Ecol. Eng.*, 73, 260-269.
- 668 18. Joss, A., Zabczynski, S., Göbel, A., Hoffmann, B., Löffler, D., Mc Ardell, C.S., Ternes,
669 T.A., Thomsen, A., Siegrist, H., 2006. Biological degradation of pharmaceuticals in
670 municipal wastewater treatment: Proposing a classification scheme. *Water Res.*, 40 (8),
671 1686-1696.
- 672 19. Li, J., Zhang, Y., Huang, Q., Shi, H., Yang, Y., Gao, S., Mao, L., Yang, X., 2017.
673 Degradation of organic pollutants mediated by extracellular peroxidase in simulated
674 sunlit humic waters: A case study with 17 β -estradiol. *J. Hazard. Mater.*, 331, 123-131.
- 675 20. Liang, S.H., Liu, J.K., Lee, K.H., Kuo, Y.C., Kao, C.M., 2011. Use of specific gene
676 analysis to assess the effectiveness of surfactant-enhanced trichloroethylene
677 cometabolism. *J. Hazard. Mater.*, 198, 323-330.
- 678 21. Luo, Y., Guo, W., Ngo, H.H., Nghiem, L.D., Hai, F.I., Zhang, J., Liang, S., Wang, X.C.,
679 2014. A review on the occurrence of micropollutants in the aquatic environment and their
680 fate and removal during wastewater treatment. *Sci. Total Environ.*, 473–474, 619-641.

- 681 22. Menz, J., Olsson, O., Kümmerer, K., 2019. Antibiotic residues in livestock manure: Does
682 the EU risk assessment sufficiently protect against microbial toxicity and selection of
683 resistant bacteria in the environment? *J. Hazard. Mater.*, 379, 120807.
- 684 23. Moon, M., Kim, C.W., Park, W.-K., Yoo, G., Choi, Y.-E., Yang, J.-W., 2013.
685 Mixotrophic growth with acetate or volatile fatty acids maximizes growth and lipid
686 production in *Chlamydomonas reinhardtii*. *Algal Res.*, 2 (4), 352-357.
- 687 24. Moussavi, G., Abbaszadeh Haddad, F., 2019. Bacterial peroxidase-mediated enhanced
688 biodegradation and mineralization of bisphenol A in a batch bioreactor. *Chemosphere*,
689 222, 549-555.
- 690 25. Nagarajan, D., Lee, D.-J., Chen, C.-Y., Chang, J.-S., 2020. Resource recovery from
691 wastewaters using microalgae-based approaches: A circular bioeconomy perspective.
692 *Bioresour. Technol.*, 302, 122817.
- 693 26. Nguyen, L.N., Hai, F.I., Kang, J., Leusch, F.D.L., Roddick, F., Magram, S.F., Price,
694 W.E., Nghiem, L.D., 2014. Enhancement of trace organic contaminant degradation by
695 crude enzyme extract from *Trametes versicolor* culture: Effect of mediator type and
696 concentration. *J. Taiwan Inst. Chem. E.*, 45 (4), 1855-1862.
- 697 27. Ni, B.-J., Fang, F., Xie, W.-M., Sun, M., Sheng, G.-P., Li, W.-H., Yu, H.-Q., 2009.
698 Characterization of extracellular polymeric substances produced by mixed
699 microorganisms in activated sludge with gel-permeating chromatography, excitation-
700 emission matrix fluorescence spectroscopy measurement and kinetic modeling. *Water*
701 *Res.*, 43 (5), 1350-1358.
- 702 28. Orvos, D.R., Versteeg, D.J., Inauen, J., Capdevielle, M., Rothenstein, A., Cunningham,
703 V., 2002. Aquatic toxicity of triclosan. *Environ. Toxicol. Chem.*, 21 (7), 1338-49.
- 704 29. Park, J., Yamashita, N., Wu, G., Tanaka, H., 2017. Removal of pharmaceuticals and
705 personal care products by ammonia oxidizing bacteria acclimated in a membrane

- 706 bioreactor: Contributions of cometabolism and endogenous respiration. *Sci. Total*
707 *Environ.*, 605-606, 18-25.
- 708 30. Perez-Garcia, O., Escalante, F.M.E., de-Bashan, L.E., Bashan, Y., 2011. Heterotrophic
709 cultures of microalgae: Metabolism and potential products. *Water Res.*, 45 (1), 11-36.
- 710 31. Sarma, H., Nava, A.R., Manriquez, A.M.E., Dominguez, D.C., Lee, W.-Y., 2019.
711 Biodegradation of bisphenol A by bacterial consortia isolated directly from river
712 sediments. *Environ. Technol. Inn.*, 14, 100314.
- 713 32. Sun, C., Dudley, S., Trumble, J., Gan, J., 2018. Pharmaceutical and personal care
714 products-induced stress symptoms and detoxification mechanisms in cucumber plants.
715 *Environ. Pollut.*, 234, 39-47.
- 716 33. Tang, J., Siegfried, B.D., Hoagland, K.D., 1998. Glutathione-S-Transferase and in Vitro
717 Metabolism of Atrazine in Freshwater Algae. *Pestic. Biochem. Physiol.*, 59 (3), 155-161.
- 718 34. Tavares, T.S., Torres, J.A., Silva, M.C., Nogueira, F.G.E., da Silva, A.C., Ramalho, T.C.,
719 2018. Soybean peroxidase immobilized on δ -FeOOH as new magnetically recyclable
720 biocatalyst for removal of ferulic acid. *Biopro. Biosys. Eng.*, 41 (1), 97-106.
- 721 35. Tran, N.H., Urase, T., Ngo, H.H., Hu, J., Ong, S.L., 2013. Insight into metabolic and
722 cometabolic activities of autotrophic and heterotrophic microorganisms in the
723 biodegradation of emerging trace organic contaminants. *Bioresour. Technol.*, 146, 721-
724 731.
- 725 36. Tu, Z., Liu, L., Lin, W., Xie, Z., Luo, J., 2018. Potential of using sodium bicarbonate as
726 external carbon source to cultivate microalga in non-sterile condition. *Bioresour.*
727 *Technol.*, 266, 109-115.
- 728 37. Vergnes, J.B., Gernigon, V., Guiraud, P., Formosa-Dague, C., 2019. Bicarbonate
729 Concentration Induces Production of Exopolysaccharides by *Arthrospira platensis* That

- 730 Mediate Bioflocculation and Enhance Flotation Harvesting Efficiency. ACS Sustain.
731 Chem. Eng., 7 (16), 13796-13804.
- 732 38. Vo Hoang Nhat, P., Ngo, H.H., Guo, W.S., Chang, S.W., Nguyen, D.D., Nguyen, P.D.,
733 Bui, X.T., Zhang, X.B., Guo, J.B., 2018. Can algae-based technologies be an affordable
734 green process for biofuel production and wastewater remediation? Bioresour. Technol.,
735 256, 491-501.
- 736 39. Vo, H.N.P., Koottatep, T., Chapagain, S.K., Panuvatvanich, A., Polprasert, C., Nguyen,
737 T.M.H., Chaiwong, C., Nguyen, N.L., 2019a. Removal and monitoring acetaminophen-
738 contaminated hospital wastewater by vertical flow constructed wetland and peroxidase
739 enzymes. J. Environ. Manage., 250, 109526.
- 740 40. Vo, H.N.P., Ngo, H.H., Guo, W., Liu, Y., Chang, S.W., Nguyen, D.D., Nguyen, P.D.,
741 Bui, X.T., Ren, J., 2019b. Identification of the pollutants' removal and mechanism by
742 microalgae in saline wastewater. Bioresour. Technol., 275, 44-52.
- 743 41. Vo, H.N.P., Ngo, H.H., Guo, W., Liu, Y., Chang, S.W., Nguyen, D.D., Zhang, X., Liang,
744 H., Xue, S., 2020. Selective carbon sources and salinities enhance enzymes and
745 extracellular polymeric substances extrusion of *Chlorella* sp. for potential co-
746 metabolism. Bioresour. Technol., 303, 122877.
- 747 42. Wang, Q., Duan, Y.-J., Wang, S.-P., Wang, L.-T., Hou, Z.-L., Cui, Y.-X., Hou, J., Das,
748 R., Mao, D.-Q., Luo, Y., 2020. Occurrence and distribution of clinical and veterinary
749 antibiotics in the faeces of a Chinese population. J. Hazard. Mater., 383, 121129.
- 750 43. Wang, S., Poon, K., Cai, Z., 2018. Removal and metabolism of triclosan by three
751 different microalgal species in aquatic environment. J. Hazard. Mater., 342, 643-650.
- 752 44. Wang, S., Wu, Y., Wang, X., 2016. Heterotrophic cultivation of *Chlorella pyrenoidosa*
753 using sucrose as the sole carbon source by co-culture with *Rhodotorula glutinis*.
754 Bioresour. Technol., 220, 615-620.

- 755 45. Xiao, R., Zheng, Y., 2016. Overview of microalgal extracellular polymeric substances
756 (EPS) and their applications. *Biotechnol. Adv.*, 34 (7), 1225-1244.
- 757 46. Xiong, J.-Q., Kim, S.-J., Kurade, M.B., Govindwar, S., Abou-Shanab, R.A.I., Kim, J.-R.,
758 Roh, H.-S., Khan, M.A., Jeon, B.-H., 2019. Combined effects of sulfamethazine and
759 sulfamethoxazole on a freshwater microalga, *Scenedesmus obliquus*: toxicity,
760 biodegradation, and metabolic fate. *J. Hazard. Mater.*, 370, 138-146.
- 761 47. Xiong, J.-Q., Kurade, M.B., Abou-Shanab, R.A.I., Ji, M.-K., Choi, J., Kim, J.O., Jeon,
762 B.-H., 2016. Biodegradation of carbamazepine using freshwater microalgae
763 *Chlamydomonas mexicana* and *Scenedesmus obliquus* and the determination of its
764 metabolic fate. *Bioresour. Technol.*, 205, 183-190.
- 765 48. Xiong, J.-Q., Kurade, M.B., Jeon, B.-H., 2018. Can Microalgae Remove Pharmaceutical
766 Contaminants from Water? *Trends Biotechnol.*, 36(1), 30-44.
- 767 49. Xiong, J.-Q., Kurade, M.B., Kim, J.R., Roh, H.-S., Jeon, B.-H., 2017. Ciprofloxacin
768 toxicity and its co-metabolic removal by a freshwater microalga *Chlamydomonas*
769 *mexicana*. *J. Hazard. Mater.*, 323, 212-219.
- 770 50. Yang, C., Hua, Q., Shimizu, K., 2000. Energetics and carbon metabolism during growth
771 of microalgal cells under photoautotrophic, mixotrophic and cyclic light-
772 autotrophic/dark-heterotrophic conditions. *Biochem. Eng. J.*, 6 (2), 87-102.
- 773 51. Yeh, K.-L., Chang, J.-S., 2012. Effects of cultivation conditions and media composition
774 on cell growth and lipid productivity of indigenous microalga *Chlorella vulgaris* ESP-31.
775 *Bioresour. Technol.*, 105, 120-127
- 776 52. Yu, Y., Han, P., Zhou, L.-J., Li, Z., Wagner, M., Men, Y., 2018. Ammonia
777 Monooxygenase-Mediated Cometabolic Biotransformation and Hydroxylamine-
778 Mediated Abiotic Transformation of Micropollutants in an AOB/NOB Coculture.
779 *Environ. Sci. Technol.*, 52 (16), 9196-9205.

- 780 53. Zhang, W., Zhang, P., Sun, H., Chen, M., Lu, S., Li, P., 2014. Effects of various organic
781 carbon sources on the growth and biochemical composition of *Chlorella pyrenoidosa*.
782 *Bioresour. Technol.*, 173, 52-58.
- 783 54. Zhao, X., Du, P., Cai, Z., Wang, T., Fu, J., Liu, W., 2018. Photocatalysis of bisphenol A
784 by an easy-settling titania/titanate composite: Effects of water chemistry factors,
785 degradation pathway and theoretical calculation. *Environ. Pollut.*, 232, 580-590.
- 786 55. Zhou, L.-J., Han, P., Yu, Y., Wang, B., Men, Y., Wagner, M., Wu, Q.L., 2019.
787 Cometabolic biotransformation and microbial-mediated abiotic transformation of
788 sulfonamides by three ammonia oxidizers. *Water Res.*, 159, 444-453.

1 **List of tables**

- 2 Table 1. Element percentages of C, N and P and C:N:P ratios in microalgae cells feed by different carbon sources, cultured with TC, SMX and
 3 BPA (each 20 µg/L).

| Elements | Carbon sources* | | | | | | | | Redfield ratio |
|----------|-----------------|------------|------------|------------|------------|------------|-------------|------------|----------------|
| | Methanol | Ethanol | Saccharose | Glucose | Acetate | Glycine | Bicarbonate | Control | |
| C | 28.4 (2.5) | 33.9 (3.2) | 46.7 (2.9) | 57.6 (3.8) | 51.7 (4.2) | 52.2 (1.9) | 48.2 (1.8) | 33.5 (2.1) | |
| N | 8.7 (0.4) | 9.2 (0.3) | 7.4 (0.7) | 9.5 (0.5) | 11.9 (1.2) | 13.6 (0.7) | 9.1 (0.3) | 9.4 (0.5) | |
| P | 2.6 (0.2) | 1.1 (0.08) | 0.3 (0.05) | 0.3 (0.02) | 0.3 (0.04) | 0.2 (0.01) | 0.4 (0.02) | 1.5 (0.1) | |
| C:N:P | 50:16:1 | 57:16:1 | 99:16:1 | 97:16:1 | 69:16:1 | 61:16:1 | 85:16:1 | 59:16:1 | 106:16:1 |

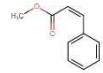
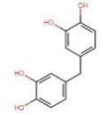
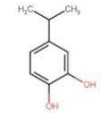
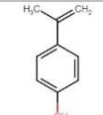
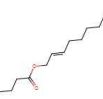
- 4 *All measures showed significant differences ($p < 0.01$). Numbers in brackets are standard deviation (SD).

Table 2. Estimated MPs cometabolism rate ($K_{\text{cometabolism}}$) (1/d) of microalgae feeding by carbon sources.

| Carbon sources | Methanol | Ethanol | Saccharose | Glucose | Acetate | Glycine | Bicarbonate | Control |
|----------------|----------|---------|------------|---------|---------|---------|-------------|---------|
| TC | 0.5 | 0.42 | 0.4 | 0.47 | 0.02 | 0.3 | 0.09 | 0.05 |
| SMX | 0.14 | 0.04 | 0.27 | 0.17 | 0.06 | 0.06 | 0.25 | 0.05 |
| BPA | 0.09 | 0.16 | 0.1 | 0.38 | 0.3 | 0.43 | 0.16 | 0.03 |

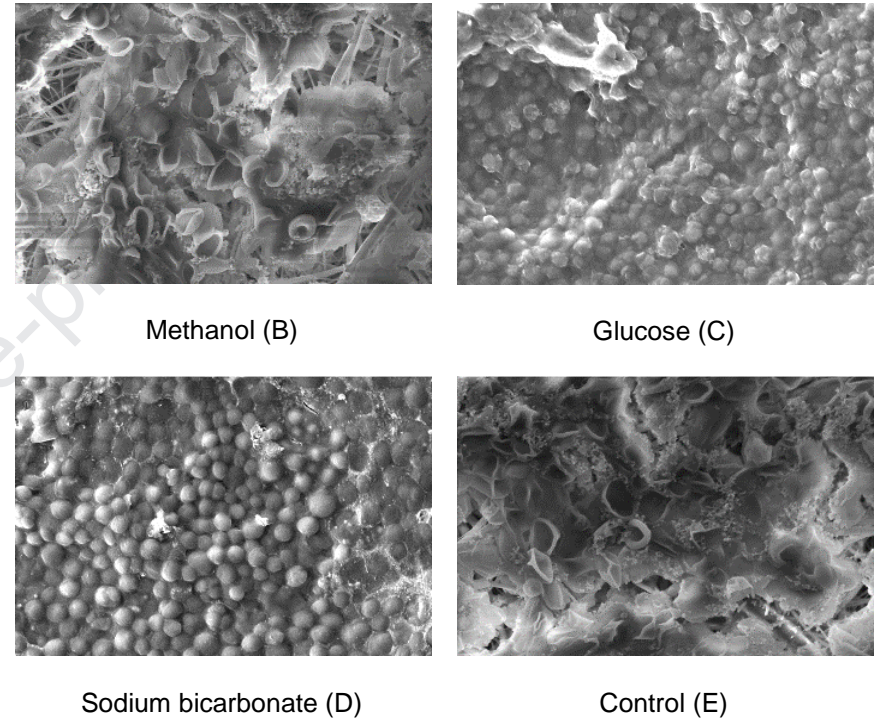
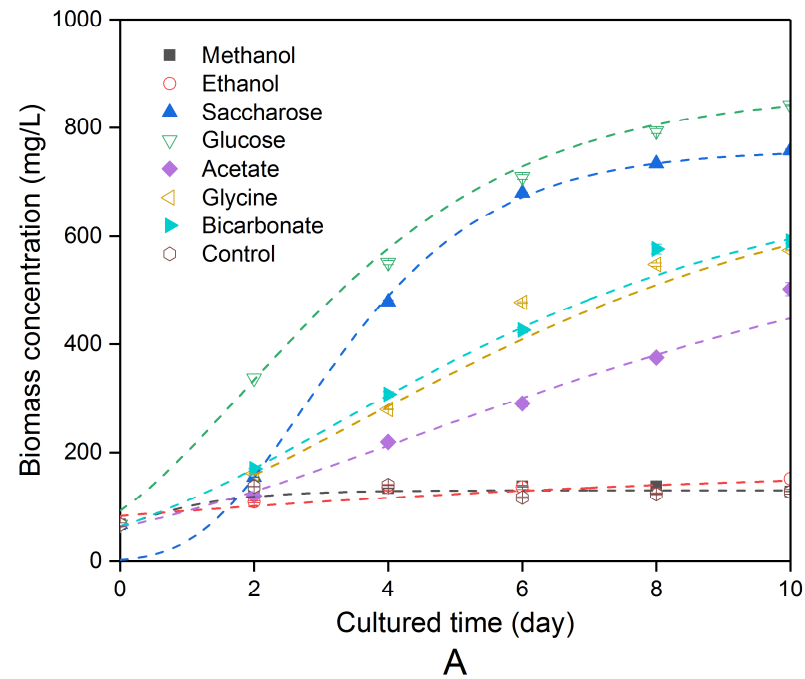
*All measures showed significant differences ($p < 0.01$).

Table 3. Degradation products of the used MPs inducing by cometabolism

| Name | Environment | Degradation product of | Formula | Recorded m/z | Retention time (min) | Peak area | Peak area in the blank sample | Possible structure |
|----------------------------------|---------------|------------------------|--|--------------|----------------------|-----------|-------------------------------|---|
| Positive mode | | | | | | | | |
| Methyl Cinnamate | Extracellular | BPA | C ₁₀ H ₁₀ O ₂ | 163.07 | 8.58 | 6.82E6 | N/A |  |
| 6,6'-diOH-BPA | Intracellular | BPA | C ₁₅ H ₁₆ O ₄ | 261.11 | 8.65 | 9.89E5 | N/A |  |
| BPA degradation product D | Intracellular | BPA | C ₉ H ₁₂ O ₂ | 153.09 | 4.77 | 5.76E5 | N/A |  |
| Negative mode | | | | | | | | |
| 4-isopropenylphenol | Extracellular | BPA | C ₉ H ₁₀ O | 133.06 | 7.72 | 2.34E7 | N/A |  |
| Valeric acid, undec-2-enyl ester | Intracellular | BPA | C ₁₆ H ₃₀ O ₂ | 253.21 | 12.34 | 4.67E7 | N/A |  |

Journal Pre-proof

1 List of figures



2 Fig. 1. Biomass growth of *Chlorella* sp. (A) and selected SEM images of microalgae feeding by different carbon sources: methanol (B), glucose
 3 (C), sodium bicarbonate (D) and control (E). The reactors were dosed TC, SMX and BPA (each 20 $\mu\text{g/L}$). All measures showed significant
 4 differences ($p < 0.01$) amongst carbon sources. Dash lines represent fitted curves of Gompertz model: $y = a \cdot e^{-\exp(-k(x-x_c))}$. Where, y is the

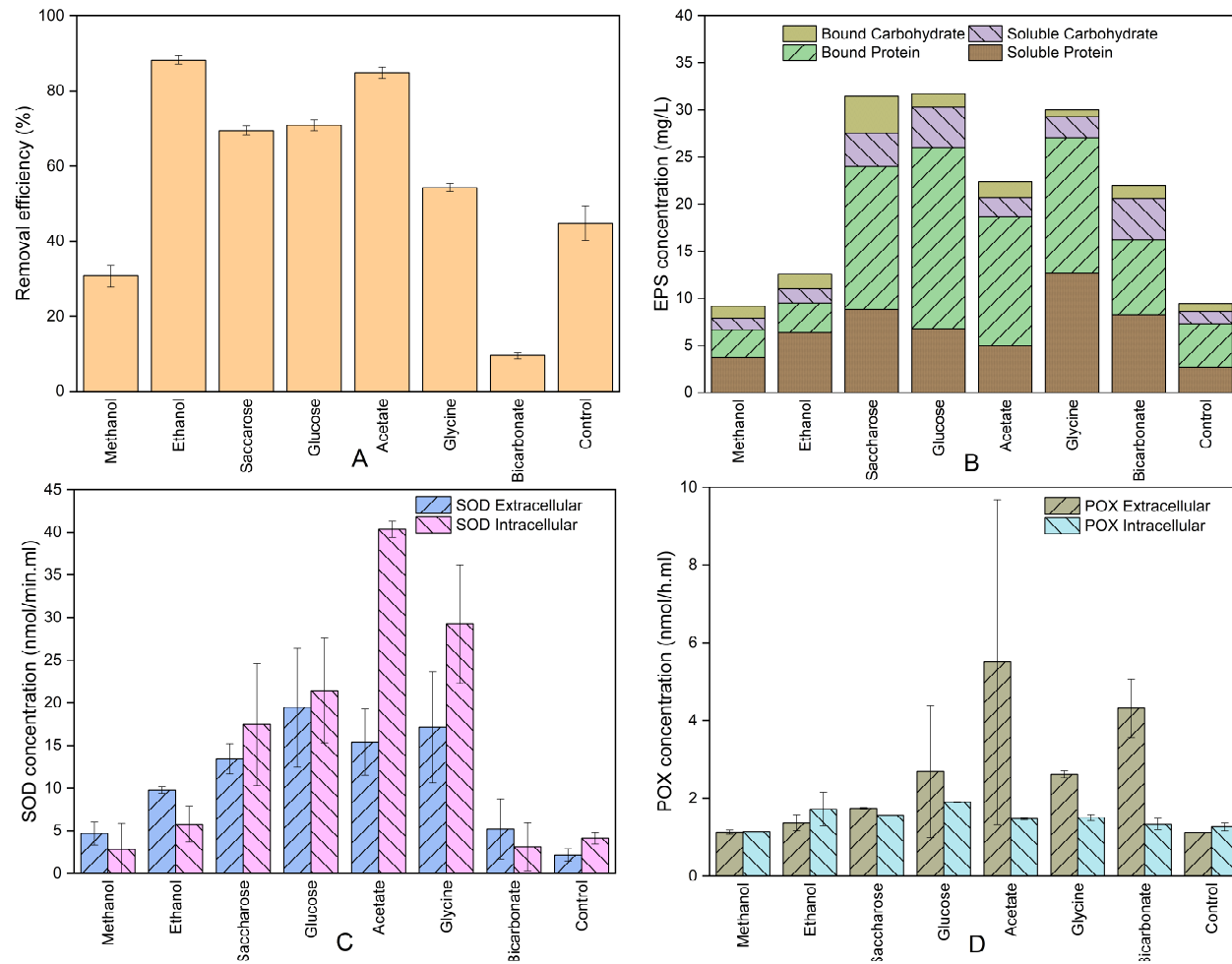
5 biomass yield (mg/L), a presents maximum biomass yield (mg/L), k presents biomass yield per day (mg/L.d), x presents cultured time (d), x_c

6 presents lag time of biomass yield (d).

7

Journal Pre-proof

8



9

10 Fig. 2. Total carbon removal efficiencies (panel A), concentrations of EPS (panel B), SOD (panel C) and POX (panel D) enzyme of *Chlorella* sp.

11 at day 10th feeding by different carbon sources, cultured with TC, SMX and BPA (each 20 μ g/L). Removal (%) = $(C_0 - C_t) / C_0 \times 100\%$. C_t

12 represents the concentrations of carbon sources at time T, C_0 represents the concentrations of carbon sources at the initial time. All measures
13 show significant differences ($p < 0.01$). The x axis of all panels performs carbon sources. The y axis presents removal efficiency (%) (panel A)
14 and concentration (panel B, C, D) ($n=2$). Notes: the scales of y axis of panels B, C and D are different.

Journal Pre-proof

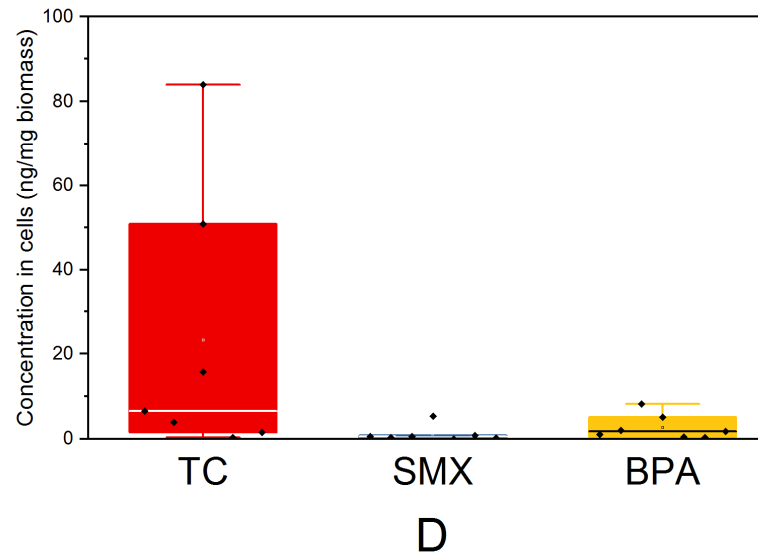
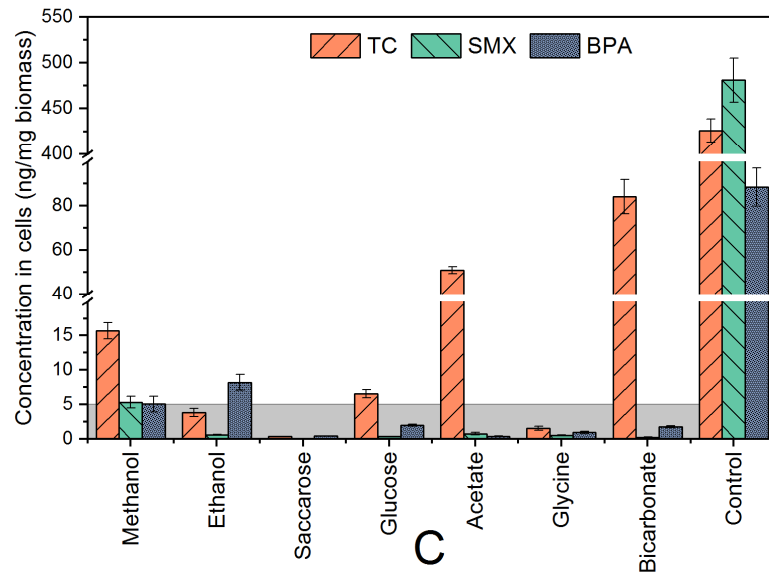
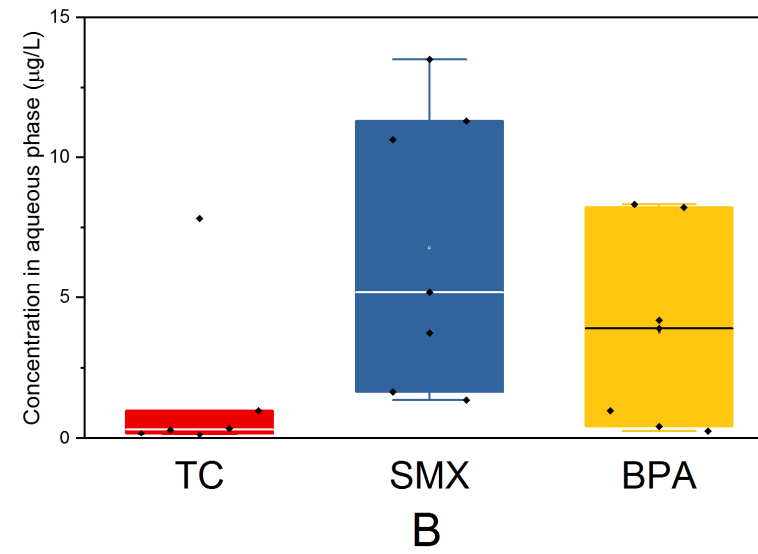
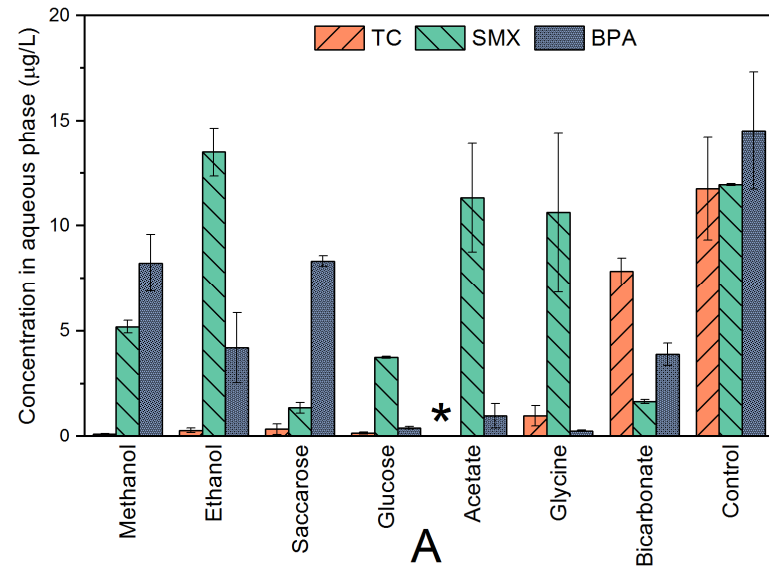


Fig. 3. Concentrations of MPs in the aqueous phase, expressed by each carbon source (panel A) and sum of all carbon sources (panel B). Concentrations of MPs in microalgae cell, expressed by each carbon source (panel C) and sum of all carbon sources (panel D). All measures show significant differences ($p < 0.01$). The analysed data in panel B and D is performed in box plots and does not include the control sample ($n=7$). The y axis of all panels performs concentration of MPs. The x axis presents carbon sources (panel A & C) and MPs (panel B & D). The value being marked with * is not reported due to improper mass balance. The values in the shade of panel C are below 5 ng/mg biomass.

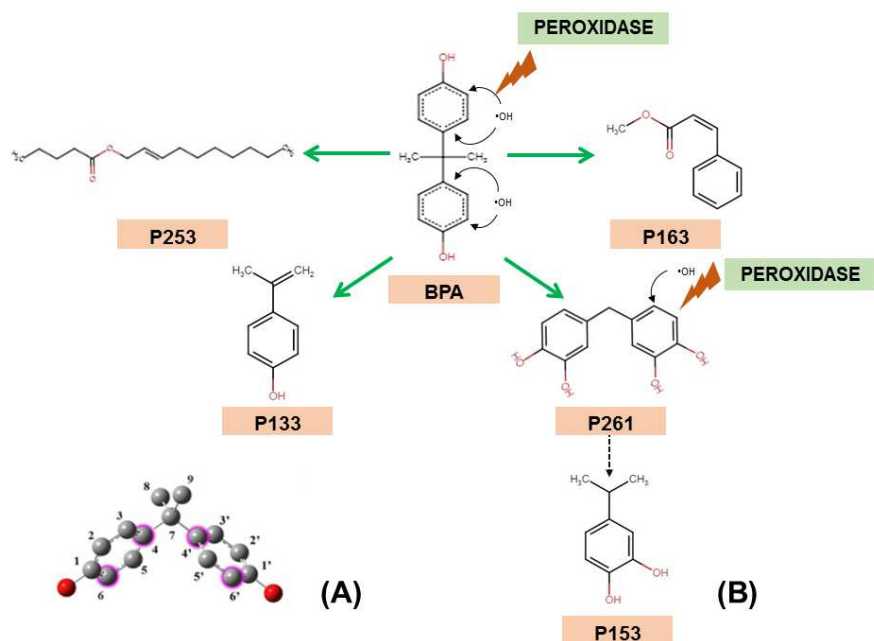


Fig. 4. Chemical structure of BPA (A) and proposed BPA degradation pathways scavenged by $\bullet\text{OH}$ group (B). The chemical structure is retrieved from Zhao et al. (2018) and performed in quantum visualization. The C atoms in pink (number 4 and 6) are the weakest in the aromatic ring and easily encountered by scavengers.

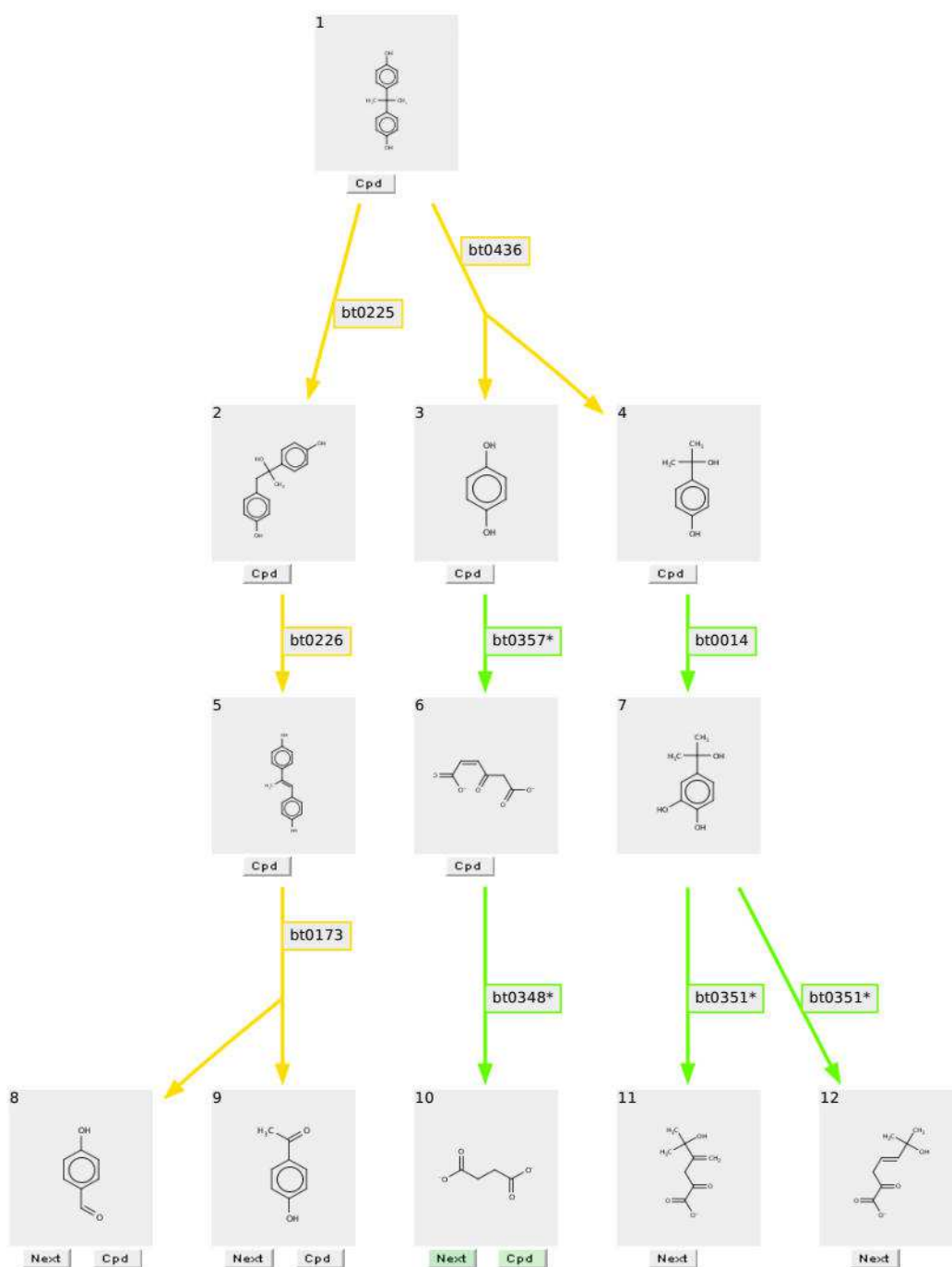


Fig. 5. Proposed BPA degradation pathway by Eawag BBD. The “btxxx” stands for the code of particular enzyme in Eawag database. Colour of the arrow presents the likelihood of degradation products formation. The green colour is “likely”. The yellow colour is “neutral”.